An Optimized Procedure for the Synthesis of AlSBA-15 with Large Pore Diameter and High Aluminum Content

A. Vinu,*,†,‡ V. Murugesan,§ Winfried Böhlmann,⊥ and Martin Hartmann†

Department of Chemistry, Chemical Technology, Kaiserslautern University of Technology, P.O. Box 3049, D-67653, Kaiserslautern, Germany; International Center for Young Scientists, National Institute for Materials Science, 1-1, Namiki, Tsukuba 305-0044, Japan; Department of Chemistry, Anna University, Chennai-600025, India; and Fakultät für Physik und Geowissenschaften, Universität Leipzig, Linnestr. 5, D-04103 Leipzig, Germany

Received: April 10, 2004; In Final Form: May 19, 2004

A series of AlSBA-15 materials with different n_{Si}/n_{Al} ratio have been synthesized by simply adjusting the molar water to hydrochloric acid ratio (n_{H_2O}/n_{HCl}). It was possible to control the n_{Si}/n_{Al} ratio, location, and coordination of Al atom in the SBA-15 silica matrix by the above method. Moreover, AlSBA-15 with n_{Si}/n_{Al} ratio up to 7 can be successfully prepared by adjusting the n_{Si}/n_{Al} ratio in the synthesis gel at n_{H_2O}/n_{HCl} of 276. The effect of the nature of Al source in the AlSBA-15 synthesis has been investigated using different aluminum source, viz., aluminum sulfate, aluminum nitrate, aluminum hydroxide, and aluminum isopropoxide. Aluminum isopropoxide was found to be the good aluminum source for AlSBA-15 material synthesis and enhanced the amount of aluminum incorporation, location, and coordination in the SBA-15 silica walls. The effect of synthesis temperature of AlSBA-15 materials has also been reported. Nitrogen adsorption measurement shows that the pore diameter of AlSBA-15 can be tuned from 9.7 to 12.5 nm by simply adjusting crystallization temperature from 100 to 130 °C. The pore volume increases from 1.35 to 1.55 cm^3/g with a concomitant decrease of the surface area from 930 to 783 m^2/g. For the first time, the mechanical stability of hexagonal AlSBA-15 materials was studied by applying different pelletizing pressures and subsequent characterization by XRD, N_2 adsorption, and mercury porosimetry. *n*-Heptane adsorption isotherms were recorded to evaluate the uptake of organics of the compressed materials. It has been found that mechanical stability of AlSBA-15 is lower compared to that of pure silica SBA-15 materials.

Introduction

The discovery of the new family of mesoporous silica molecular sieves with pore diameters in the 2.0−10.0 nm range, designated as M41S, is of considerable interest for heterogeneous catalysis and material science.[1,2] This family of materials is characterized by a regular array of pores with uniform diameter, high specific surface areas, and pore volumes which are advantageous for the adsorption and conversion of bulky molecules. However, the materials consisting of pure silica frameworks are of limited use for various catalytic applications because of the lack of acid sites and ion-exchange capacity.

The ability to tailor the pore structure and control the chemical composition of these materials represents a timely topic in catalysis research. The incorporation of Al and other transition-metal elements into the amorphous silica walls is mandatory for the formation of a catalytically active site in mesoporous molecular sieves.[3,4] Depending on the nature and number of trivalent framework cations, both strength and density of the acid sites may be varied. Mesoporous molecular sieves of the M41S family are promising catalysts for a variety of reactions such as alkylation of aromatics,[5] hydrocarbon cracking,[6] and upgrading of heavy oil. However, these materials lack thermal and hydrothermal stability due to their thin walls and are typically less acidic as compared to conventional zeolite cracking catalyst.[7] Many efforts have been made to improve the thermal and hydrothermal stability of mesosporous molecular sieves,[8−10] e.g., by thickening or crystallizing the pore walls.[11−13]

Highly ordered large pore mesoporous silica molecular sieves SBA-15 with considerably thicker pore walls as compared to MCM-41 have been recently synthesized using an amphiphilic triblock copolymer as the structure directing agent in highly acidic media.[8,14−16] SBA-15 exhibits improved hydrothermal stability as compared to MCM-41.[1,16] The incorporation of aluminum into SBA-15 by postsynthetic and direct methods has been reported.[17−22] During materials preparation via postsynthetic methods often metal oxides are formed in the channels or on the external surface. Metal oxides formed in the mesopores will block the pores partially or fully, thereby reducing surface area, pore volume, and pore diameter, or play a negative role in catalysis.[23] Yue et al.[17] reported the direct synthesis of AlSBA-15 and found that catalytic activity of AlSBA-15 in cumene cracking is higher as compared to AlMCM-41. However, the highly acidic synthesis gel required for the formation of SBA-15 limits the direct incorporation of high amounts of trivalent metal ions into the neutral silica framework and requires a postsynthetic treatment to remove octahedral aluminum. A different strategy is the transformation of amorphous SBA-15 walls into crystalline aluminosilicates.[24,25] Even though the materials formed are good cracking catalysts, the synthesis procedure is somewhat tedious and requires two steps. There-

† Kaiserslautern University of Technology.
‡ National Institute for Materials Science.
§ Anna University.
⊥ Universität Leipzig.
* To whom correspondence should be addressed: Ph +81-29-851-3354 (Ext 8679); Fax +81-29-860-4706; e-mail vinu.ajayan@nims.go.jp.

10.1021/jp048411f CCC: $27.50
Published on Web 07/03/2004

fore, it is still a challenge to find a one-step route to SBA-15 materials with high Al content in order to increase the acidity without changing its structural order or increasing the complexity of the synthesis.

It has been found for AlMCM-41 that the extent of Al incorporation and substitution in the tetrahedral framework[26] and the catalytic activity[27] are greatly dependent on the Al source which are used for the preparation of these materials.[28−33] Janicke et al.[28] and Reddy and Song[31,33] have reported that Al isopropoxide is a better source for the incorporation of Al(III) in MCM-41 while Luan et al.[30] have reported Al sulfate as the best source among all other Al sources. On the contrary, Borade and Clearfield[29] have found that sodium aluminate is the source for maximum incorporation. Recently, Hartmann et al.[34] have reported the effect of Al source on the incorporation of MCM-48 and found that the maximum incorporation of Al and large pore diameter on the MCM-48 were achieved by using Al isopropoxide as the Al source. However, to the best of our knowledge, the effect of various Al sources in the SBA-15 synthesis has not been reported in the open literature so far.

Materials with uniform and tunable pore sizes are expected to play an important role in a number of applications that range from catalysis, to molecular separations and sorption of very bulky molecules,[35] and to the fabrication of semiconductors, semiconductor nanowires, and low dielectric devices.[36,37] Recently, we have reported the synthesis of pure silica SBA-15 with different pore diameters by simply adjusting the synthesis temperature between 100 and 150 °C. However, tuning the pore size of Al substituted SBA-15 has not been reported up until now.

In the present contribution, we report an optimized procedure for the synthesis of high Al content SBA-15 molecular sieves including an adjustment of the n_{H_2O}/n_{HCl} ratio in order to lower the pH of the synthesis medium. Al isopropoxide was found to be the preferred Al source among all Al sources studied. The pore diameter of AlSBA-15 can be tuned from 9 to 13 nm by simply adjusting the crystallization temperature without addition of any organic swelling agents. Furthermore, the mechanical stability of hexagonal AlSBA-15 materials was studied by applying different pelletizing pressures and subsequent characterization by XRD and N_2 adsorption. *n*-Heptane adsorption isotherms were recorded to evaluate the uptake of organics of the compressed materials. It has been found that mechanical stability of AlSBA-15 is lower compared to that of pure silica SBA-15 materials.

Experimental Section

Synthesis. AlSBA-15 was synthesized using a triblock copolymer poly(ethylene glycol)-*block*-poly(propylene glycol)-*block*-poly(ethylene glycol) (Pluronic P123, molecular weight = 5800, $EO_{20}PO_{70}EO_{20}$, Aldrich) as a structure directing agent. In a typical synthesis, 4 g of Pluronic P123 was added to 30 mL of water. After stirring for a few hours, a clear solution was obtained. Thereafter, the required amount of HCl was added, and the solution was stirred for another 2 h. Then, 9 g of tetraethyl orthosilicate and the required amount of the desired Al source were added, and the resulting mixture was stirred for 24 h at 313 K. A first set of samples was prepared by changing the molar water to hydrochloric acid ratio and denoted as AlSBA-15(*x*H), where *x* denotes the molar water to hydrochloric acid ratio (n_{H_2O}/n_{HCl}). For this set of samples, the n_{Si}/n_{Al} ratio in the gel was fixed to 7. A second set of samples was prepared by using a fixed molar water to hydrochloric acid ratio of 276 (70 mL of 0.29 M HCl) and a n_{Si}/n_{Al} ratio of 7 while varying the Al source. These samples are denoted AlSBA-15(AS), -(AN), -(AH), and -(A*i*Pr) where AS, AN, AH, and A*i*Pr are the abbreviated form of Al sulfate, Al nitrate, Al hydroxide, and Al isopropoxide, respectively. A third set of AlSBA-15 samples with n_{Si}/n_{Al} ratio of 7 was prepared by varying the synthesis temperature from 100 to 130 °C. The samples were labeled AlSBA-15(*y*T), where *y* denotes the synthesis temperature. The solid products were recovered by filtration, washed several times with water, and dried overnight at 373 K. The molar gel composition was 1 TEOS:0.02−0.15 Al_2O_3:0.016 P123:0.46−5.54 HCl:127−190 H_2O. Finally, the samples were calcined at 813 K to remove the template.

Characterization. The powder X-ray diffraction patterns of the AlSBA-15 materials were collected on a Siemens D5005 diffractometer using Cu Kα (λ = 0.154 nm) radiation. The diffractograms were recorded in the 2θ range of 0.8° to 10° with a 2θ step size of 0.01° and a step time of 10 s. Nitrogen adsorption and desorption isotherms were measured at 77 K on a Quantachrome Autosorb 1 sorption analyzer. All samples were outgassed for 3 h at 250 °C under vacuum ($p < 10^{-5}$ hPa) in the degas port of the sorption analyzer. The specific surface area was calculated using the BET model. The pore size distributions were obtained from the adsorption branch of the nitrogen isotherms using the Barrett−Joyner−Halenda method.

Solid-state ^{27}Al MAS NMR spectra were recorded at room temperature on a Bruker MSL 500 NMR spectrometer at a resonance frequency of 130.32 MHz, applying a short 2.1 μs pulse (π/6) and a recycle delay of 100 ms. The samples were spun at 10 kHz using a 4 mm diameter zirconia rotor. Up to 12 500 scans were necessary to obtain a satisfactory signal-to-noise ratio.

To test the mechanical stability of the AlSBA-15 material with the n_{Si}/n_{Al} ratio of 7, the above calcined samples were compressed in a steel die of 24 mm diameter, using a hand-operated press, for 30 min. The four different external pressure applied (0, 43, 107, and 217 MPa) were calculated from the external force applied and the diameter of the die. Subsequently, the obtained disk was crushed and sieved to obtain pellets with a diameter of 0.2−0.35 nm, which were used for all further measurements. The pressed samples were denoted as AlSBA-15(*p*MPa), where *p* specifies the pressure in MPa. *n*-Heptane adsorption isotherms were recorded using a home-built volumetric adsorption apparatus. Prior to the adsorption experiments, the samples were dehydrated at 200 °C under vacuum ($p < 10^{-6}$ hPa) for 4 h.

Results and Discussion

Variation of the Water to Hydrochloric Acid Molar Ratio (n_{H_2O}/n_{HCl}). As the SBA-15 hexagonal phase is synthesized under highly acidic condition ($n_{H_2O}/n_{HCl} < 33$, i.e., pH < 1), it is difficult to synthesize its aluminum-containing form due to the high solubility of aluminum precursors, which hinders their incorporation into the silica walls of SBA-15. Therefore, we have tried to increase the amount of Al incorporation by simply adjusting the n_{H_2O}/n_{HCl} ratio of the gel without changing the structural integrity of parent SBA-15 materials. The initial n_{Si}/n_{Al} ratio was fixed to 7. The powder XRD patterns of aluminosilicate SBA-15 samples prepared using different water to hydrochloric acid (HCl) molar ratios n_{H_2O}/n_{HCl} are shown in Figure 1. The well-defined XRD patterns are similar to those recorded for all-silica SBA-15 materials as described by Zhao et al.[8] The XRD pattern of all AlSBA-15 materials exhibit five well-resolved peaks which are indexed to the (100), (110), (200), (210), and (300) reflections of the hexagonal space group *p*6*mm*.

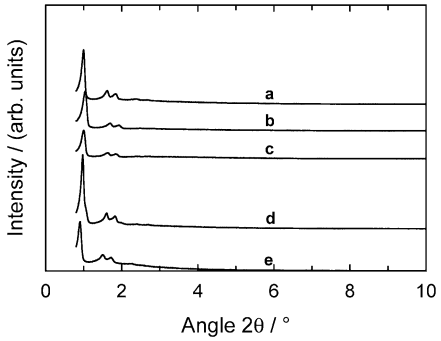

Figure 1. XRD powder patterns of AlSBA-15 materials prepared at different n_{H_2O}/n_{HCl} ratios: (a) AlSBA-15(276H), (b) AlSBA-15(137H), (c) AlSBA-15(68H), (d) AlSBA-15(33H), and (e) SBA-15(33H).

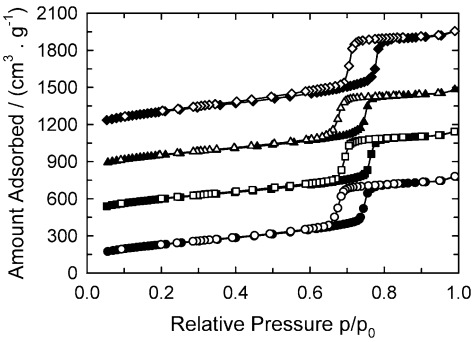

Figure 2. Nitrogen adsorption isotherms of AlSBA-15 materials prepared at different n_{H_2O}/n_{HCl} ratios (closed symbols, adsorption; open symbols, desorption): (●) AlSBA-15(276H), (■) AlSBA-15(137H), (▲) AlSBA-15(68H), and (◆) AlSBA-15(33H).

The length of the hexagonal unit cell a_0 is calculated using the formula $a_0 = 2d_{100}/\sqrt{3}$. The observed d spacings are compatible with the hexagonal $p6mm$ space group. The length of the unit cell a_0 increases from 9.98 to 11.27 with increasing n_{H_2O}/n_{HCl} molar ratio from 33 to 276. Moreover, it is found that the n_{Si}/n_{Al} ratio of the product decreases from 574 to 45 with increasing n_{H_2O}/n_{HCl} ratio. The above described experiments suggest that the amount of Al incorporation can be controlled by simply adjusting the molar n_{H_2O}/n_{HCl} ratio without affecting the structural order of the parent SBA-15 materials.

Information on the textural properties of porous solids are typically obtained from low-temperature (77 K) nitrogen adsorption isotherms, which allow calculation of the specific surface area, specific pore volume, and mesopore size distribution. The nitrogen adsorption−desorption isotherms are shown in Figure 2, and the textural properties are collected in Table 1. All isotherms are of type IV according to the IUPAC classification and exhibited a H1-type broad hysteresis loop, which is typical of large-pore mesoporous solids.[38] As the relative pressure increases ($p/p_0 > 0.6$), all isotherms exhibit a sharp step characteristic of capillary condensation of nitrogen within uniform mesopores, where the p/p_0 position of the inflection point is correlated to the diameter of the mesopore. As SBA-15 has a hexagonal arrangement of mesopores connected by smaller micropores,[39] it is clear that the broad hysteresis loop in the isotherms of SBA-15 reflects the long mesopores, which limit the emptying and filling of the accessible volume.

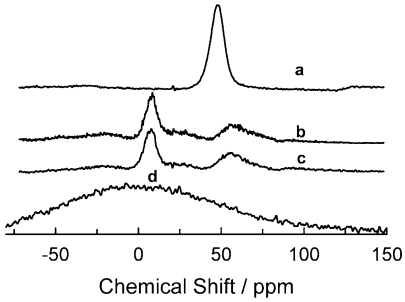

Figure 3. ^{27}Al MAS NMR spectra of AlSBA-15 materials prepared at different n_{H_2O}/n_{HCl} ratios: (a) AlSBA-15(276H), (b) AlSBA-15(137H), (c) AlSBA-15(68H), and (d) AlSBA-15(33H).

Specific surface area and specific pore volume systematically increase with increasing molar n_{H_2O}/n_{HCl} ratio. The specific surface area amounts to 833 m^2/g for AlSBA-15(33H) and increases to 930 m^2/g for AlSBA-15(276H), while the specific pore volume increases from 1.15 to 1.35 cm^3/g for the same samples. The pore diameter of AlSBA-15(276H) is 9.7 nm, which is 1.2 nm higher than for the sample prepared at very low n_{H_2O}/n_{HCl} ratio of 33. It is also interesting to note that the specific surface area, specific pore volume, and pore diameter of AlSBA-15(276H) are higher as compared to those of pure silica SBA-15 materials. All these observations suggest that a high n_{H_2O}/n_{HCl} ratio favors Al incorporation into SBA-15 without affecting the structural order.

In Figure 3a, the ^{27}Al MAS NMR spectra of the calcined AlSBA-15 samples prepared at different n_{H_2O}/n_{HCl} ratio are displayed. For AlSBA-15(276H), only a very sharp peak with a chemical shift of 47.5 ppm is observed. The peak at 47.5 ppm is assigned to Al in a tetrahedral environment (AlO_4 structural unit, Al(tet)), in which Al is covalently bound to four Si atoms via oxygen bridges. For the samples prepared with n_{H_2O}/n_{HCl} ratios of 137 and 68, two peaks with chemical shift of 0 and ca. 54 ppm, respectively, are observed. It should also be noted that AlSBA-15(33H) shows only one broad peak centered at 0 ppm. The peak at 0 ppm is assigned to octahedral Al (AlO_6 structural unit, Al(oct)).[30] The peak at at ca. 54 ppm is attributed to tetrahedrally coordinated Al atoms. These results reveal that the "efficiency" of Al incorporation increases with decreasing pH of the gel. The aluminum atoms are exclusively in tetrahedral coordination at a n_{H_2O}/n_{HCl} ratio of 276, while a reduced n_{H_2O}/n_{HCl} ratio favors octahedral coordination of Al or no incorporation at all. ^{29}Si MAS NMR spectra of calcined samples showed rather broad asymmetric signals (not shown), which can be divided into two Gaussian lines with chemical shifts close to −100 and −111 ppm for $Si(OSi)_3OH$ and $Si(OSi)_4$ groups, respectively.

The above results suggest a successful isomorphous substitution of Al into the siliceous framework of SBA-15 by a direct synthesis method using a n_{H_2O}/n_{HCl} ratio of 276. The incorporation of Al into SBA-15 under retained structural order with increasing n_{H_2O}/n_{HCl} ratio can be explained by the synthesis mechanism of SBA-15 proposed by Zhao et al.[8] According to this mechanism, the formation of hexagonal mesophase under highly acidic conditions occurs through the $S^0H^+X^-I^+$ pathway (nonionic polymeric surfactant (S^+), halogen anions (X^-), and

TABLE 1: Structural Parameters of AlSBA-15 Samples Prepared at Different n_{H_2O}/n_{HCl} Ratios

sample	n_{H_2O}/n_{HCl}	n_{Si}/n_{Al}	a_0/nm	$A_{BET}/(m^2/g)$	pore volume/(cm^3/g)	pore diameter $d_{p,\,ads}$/nm
SBA-15(33H)	33		10.14	910	1.25	9.2
AlSBA-15(33H)	33	574	9.98	833	1.15	8.5
AlSBA-15(68H)	68	458	10.32	900	1.18	8.9
AlSBA-15(137H)	137	285	10.57	916	1.17	8.5
AlSBA-15(276H)	276	45	11.27	930	1.35	9.7

TABLE 2: Textural Parameters of AlSBA-15 Samples Prepared by Using Different Aluminum Sources

sample	a_0/nm	n_{Si}/n_{Al}	$A_{BET}/(m^2/g)$	pore volume/(cm^3/g)	pore diameter $d_{p,\,ads}$/nm
AlSBA-15(AS)	9.60	258	1007	1.25	8.9
AlSBA-15(AN)	11.52	152	988	1.22	8.5
AlSBA-15(AH)	10.63	116	991	1.35	10.0
AlSBA-15(A*i*Pr)	11.27	45	930	1.35	9.7

the protonated inorganic SiO_2 species (I^+)). At very high pH, the alkylene oxide groups of the surfactant are solubilized and the hydronium ions are associated with the alkylene oxygen atoms. Since the point of zero net charge of silica is at pH = 2, the silica species are positively charged by proton abstraction at low pH. The charge-associated alkylene oxide units and the cationic silica species are assembled together by a combination of electrostatic, hydrogen bonding, and van der Waals interactions $REO_{m-y}[(EO)\cdot H_3O^+]_y...yX^-...I^+$, which can be designated as $(S^0H^+)(X^-I^+)$. As already mentioned, at high pH the introduction of aluminum is very difficult due to the high solubility of the precursors. This can be explained by the following equations:

$$Al(C_3H_7O)_{3(S)} + 3H^+_{(aq)} \rightleftharpoons Al^{3+}_{(aq)} + 3C_3H_7OH_{(aq)} \quad (1)$$

$$Al^{3+} + 2H_2O \rightarrow Al(OH)_2^+ + 2H^+ \quad (2)$$

From the above mechanism, it is clear that a high acidic medium is necessary for the formation of the hexagonal mesophase SBA-15 but prohibits the introduction of aluminum. Hence, we decided to optimize the pH of the synthesis medium by adjusting the n_{H_2O}/n_{HCl} ratio. Initially, we studied the formation of the hexagonal phase after adjusting the pH of the synthesis gel between 0 and 1.6. Once the surfactant and silica species are protonated, the cationic silica species undergo partial condensation and form mesostructure through the counteranion (X^-) with the cationic surfactant species; as a result, pH of the synthesis medium increases. It should be noted that when the n_{H_2O}/n_{HCl} ratio was increased from 33 to 137, the pH of the synthesis gel was still below 1.5 even after a few hours of stirring after addition of the silicon source. But with increasing the n_{H_2O}/n_{HCl} ratio to 276, the pH of the synthesis gel was around 2.1, which is above the zero net charge of silica. If the pH of the synthesis medium rises above the zero net charge of silica, the silica species are negatively charged which enhances the interaction with the $Al(OH)_2^+$ species. With decreasing H^+ concentration in the synthesis gel, the concentration of aluminum hydroxyl species increases (eq 2). Hence, the partially condensed silica species are able to form Al−O−Si bond with $Al(OH)_2^+$ species at high pH. Moreover, the structural order of the materials is maintained when formed at a pH of ca. 2.

Variation of the Aluminum Source. In the following set of experiments, different aluminum sources such as $Al_2(SO_4)_3$, $Al(NO_3)_3$, $Al(OH)_3$, and aluminum isopropoxide are used for the synthesis of AlSBA-15. There is a large variation in the n_{Si}/n_{Al} ratio of the final product as a function of the Al source used in the synthesis gel. The n_{Si}/n_{Al} ratios of the final AlSBA-15 materials starting from a n_{Si}/n_{Al} ratio of 7 are 258 (aluminum sulfate), 152 (aluminum nitrate), 116 (aluminum hydroxide), and 45 (aluminum isopropoxide) as determined by chemical analysis (Table 2). AlSBA-15 synthesized by using Al isopropoxide as the Al source shows the highest amount of Al incorporation. This is in agreement with the results of our previous work on AlMCM-48, which showed that the use of Al isopropoxide facilitates the incorporation of the Al into the silica walls.[34] The use of Al sulfate and Al nitrate results in a reduced pH of the synthesis gel. As reported above, a highly acidic synthesis gel is not favorable for Al incorporation; thus, the reduced pH of the synthesis gel is most likely the reason for the reduced incorporation of Al in AlSBA-15(AS) and AlSBA-15(AN).

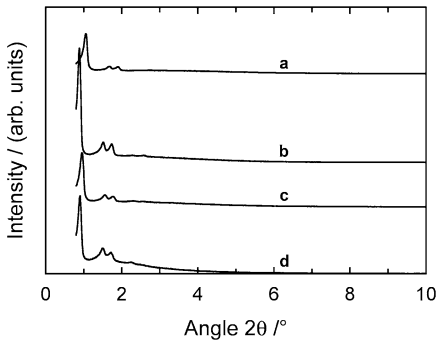

Figure 4. XRD powder patterns of AlSBA-15 materials prepared using different Al sources: (a) AlSBA-15(AS), (b) AlSBA-15(AN), (c) AlSBA-15(AH), and (d) AlSBA-15(AiPr).

The powder XRD patterns of aluminosilicate SBA-15 prepared from Al sulfate, Al nitrate, Al hydroxide, and Al isopropoxide are shown in Figure 4. The materials prepared from different Al sources show at least three well-resolved peaks which are indexed to the (100), (110), and (200) reflections of the hexagonal space group *p*6*mm*. The intensity of the XRD pattern is higher compared to the intensity of the XRD patterns observed for SBA-15 prepared from Al sulfate. The difference in the intensity of the XRD reflection with various metal sources could be due to the generation of their respective counterions such as NO_3^-, OH^-, $C_3H_7O^{3-}$, and SO_4^{2-} which would affect the interaction of the surfactant with the silicate species. The nitrate ion especially gives the strongest counterion association which neutralizes the micellar charge. The stronger charge neutralization would in turn help the formation of more rigid micelles and hence better hexagonal structure.[40,41] Thus, the intensity of the XRD pattern of AlSBA-15(AN) is higher compared to those of other AlSBA-15 materials. However, the divalent sulfate from the Al sulfate source shows somewhat different behavior and creates HSO_4^- species in the synthesis medium. This will bind only weakly to the surfactant, and hence the formation of $(S^0H^+)(X^-I^+)$ is much inhibited. Therefore, the intensity of XRD pattern of AlSBA-15(AS) and its unit cell constant are very low compared to those of other AlSBA-15 materials synthesized by using different Al source. Similar reduction in the intensity of XRD peaks and unit cell constants have been reported for AlMCM-41 synthesized using Al sulfate as the Al source.[30,42]

The nitrogen adsorption isotherms of AlSBA-15 samples prepared by using different Al sources are given in Figure 1S (see Supporting Information), and the textural parameters for the resulting samples are summarized in Table 2. All samples exhibit a high degree of structural ordering, as indicated by the steep capillary condensation step of the respective adsorption isotherm. All samples exhibit a specific surface area of more than 930 m^2/g. The samples AlSBA-15(AH) and AlSBA-15(iPr) possess specific pore volumes of 1.35 cm^3/g, whereas the pore diameter is determined to 10.0 and 9.7 nm, respectively.

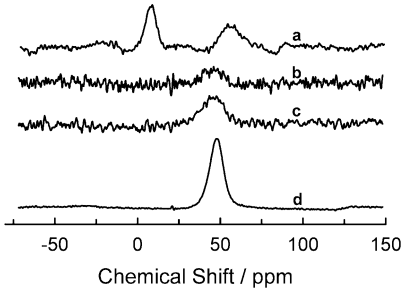

Figure 5. ^{27}Al MAS NMR spectra of AlSBA-15 materials prepared using different Al sources: (a) AlSBA-15(AS), (b) AlSBA-15(AN), (c) AlSBA-15(AH), and (d) AlSBA-15(AiPr).

Moreover, these values are significantly higher than those of AlSBA-15(AS), AlSBA-15(AN), and the parent material SBA-15. It is interesting to note that the unit cell constant $a_0 = 11.52$ nm of AlSBA-15(AN) is larger as compared to those of all other materials, while the pore diameter of the respective material is low as compared to those of other materials, which in turn leads to a larger wall thickness. It has been reported that the charge/radius (Z/r, Å^{-1}) ratio of the central cation of the anionic species controls the rate of the silica condensation.[43] It was also found that the time required for obtaining a well-ordered MCM-41 material decreases with increasing Z/r ratio. The Z/r ratio of NO_3^- is 2 times higher than SO_4^{2-}, and hence NO_3^- ion promotes more silica condensation and helps the formation of thicker wall of the hexagonal structure in the SBA-15 materials. All these observations indicate that the structural order, textural parameters, and the introduction of aluminum on the AlSBA-15 materials can be controlled by choosing different sources of Al.

The ^{27}Al MAS NMR spectra of calcined AlSBA-15 samples prepared from different aluminum sources are shown in Figure 5. It can be seen that the Al source influences both the extent of Al incorporation and the coordination of the Al in the SBA-15 walls. The calcined AlSBA-15 samples prepared by using Al hydroxide and Al nitrate showed only a broad peak centered around 46.5 and 46 ppm, respectively, whereas a sharp peak centered around 47.5 ppm was observed for AlSBA-15(iPr). These peaks are attributed to aluminum in tetrahedral coordination. However, the AlSBA-15 sample prepared by using Al sulfate showed two peaks centered around 7 and 54 ppm which are attributed to aluminum atoms in octahedral and tetrahedral coordination in the SBA-15 framework, respectively. The described results indicate that the use of aluminum isopropoxide is preferred for the synthesis of AlSBA-15 with aluminum predominantly in tetrahedral coordination.

Variation of the n_{Si}/n_{Al} Ratio. The elemental compositions of AlSBA-15 materials synthesized by using Al isopropoxide as the Al source with different n_{Si}/n_{Al} ratios are listed in Table 3. In all cases, the n_{Si}/n_{Al} ratio of the calcined materials is lower than n_{Si}/n_{Al} ratio in the synthesis gel. This could be due to the high solubility of the Al source in the acidic medium. However, AlSBA-15 materials with n_{Si}/n_{Al} ratios of 100 to 7 have been obtained.

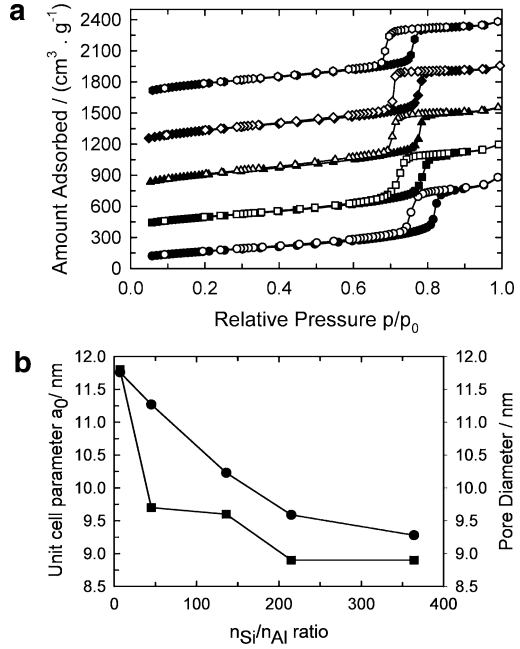

Figure 6. (a) Nitrogen adsorption isotherms of AlSBA-15 materials prepared at different Si/Al ratios (closed symbols, adsorption; open symbols, desorption): (●) AlSBA-15(7), (■) AlSBA-15(12), (▲) AlSBA-15(45), (◆) AlSBA-15(136), and (⬣) AlSBA-15(215). (b) Evolution of unit cell parameter as a function of Al propoxide content: (●) unit cell parameter and (■) pore diameter.

The powder XRD patterns of the AlSBA-15 samples synthesized by using Al isopropoxide as the Al source with different n_{Si}/n_{Al} ratios are given in Figure 2S (see Supporting Information). All samples show at least four well-resolved peaks which are indexed to the (100), (110), (200), and (210) reflections. Interestingly, the intensity of the reflections increases with decreasing n_{Si}/n_{Al} ratio, except for AlSBA-15(7). This indicates that the structural order was improved with Al incorporation into the SBA-15 framework. For the sample AlSBA-15(7), the (110) reflection is very well pronounced, whereas the intensity of the higher reflections is reduced.

Figure 6a shows the nitrogen adsorption isotherms of AlSBA-15 samples synthesized by using Al isopropoxide as the Al source with different n_{Si}/n_{Al} ratios. All isotherms show a sharp condensation step at relative pressures in the range of 0.63−0.9. It can also be seen that the capillary condensation step is shifted to higher relative pressures with increasing aluminum content in the product. This corresponds to increase of the pore diameter as the Al content of the sample increases. Moreover, with decreasing n_{Si}/n_{Al} ratio of the final product, pore diameter and unit cell size increase at the expense of the specific surface area as expected for cylindrical pores (Table 3). Unit cell size and pore diameter decrease monotonically with increasing n_{Si}/n_{Al} ratio of the product (Figure 6b). The same effect has been found when Al isopropoxide is used as the Al source in the synthesis of MCM-48.[44] It is obvious that the enlargement of the unit cell size is not a consequence of Al introduction into the walls since the unit cell size enlargement is limited to the

TABLE 3: Textural Parameters of AlSBA-15 Samples Prepared at Different n_{Si}/n_{Al} Ratio

sample	a_0/nm	gel n_{Si}/n_{Al}	n_{Si}/n_{Al}	A_{BET}/(m^2/g)	pore volume/(cm^3/g)	pore diameter $d_{p,\,ads}$/nm
AlSBA-15(7)	11.76	3	7	604	1.26	11.8
AlSBA-15(12)	11.76	5	12	719	1.30	9.7
AlSBA-15(45)	11.27	7	45	930	1.35	9.7
AlSBA-15(136)	10.23	14	136	1026	1.35	9.6
AlSBA-15(215)	9.59	27	215	1033	1.31	8.9
AlSBA-15(364)	9.28	55	364	1039	1.28	8.9

use of aluminum isopropoxide as the aluminum source. The observed pore size enlargement in AlSBA-15 prepared from aluminum isopropoxide could be explained by two ways. The first explanation is based on the micelle formation mechanism using nonionic surfactants. The driving force of the micelle formation is the transfer of the hydrophobic surfactant chain from water into the nonpolar core of the micelles. This force is opposed by steric or polar interactions between surfactant headgroups. The balance between these forces can be accounted for by a molecular packing ratio, *R*, defined as[41]

$$R = V/la \tag{3}$$

where *V* is the volume of the hydrophobic part of the surfactant, *a* is the effective headgroup area of the surfactant, and *l* is the effective length of the surfactant chain. An increase of the amount of Al isopropoxide in the synthesis gel results in the presence of a large amount of propanol in the gel. The alcohol molecules are accumulated at the micelle/water interface. The hydrocarbon chain of the propanol will be oriented into the interior part of the micelles, while polar headgroups are located preferentially at the interface.[45] The result is essentially a screening of the repulsion between the nonionic surfactants; i.e., the effective area per headgroup *a* decreases. Moreover, there will be an increase in the volume of the micelles. This increase will depend on the amount of propanol in the mixture. Hence, the numerator in the packing ratio (eq 3) will increase. At the same time, the denominator will decrease due to the reduction of *a*. Consequently, a transition into longer micelles can be predicted from the packing ratio. As a result, the pore diameter is increased with increasing the Al isopropoxide content in the synthesis gel.

The second possible explanation is the limitation of inorganic condensation in the presence of excess of propanol. The PEO side chain is hydrophilic in nature and penetrates into the walls. There hydrogen bondings with the silanol groups occur, and micropores are created inside the walls. In the presence of excess propanol, the PEO groups may also interact with propanol through hydrogen bonding. The resulting PEO−propanol moiety might also interact with silanol groups and penetrate the SBA-15 walls. Moreover, it is believed that the incorporation of large amounts of Al and excess of alcohol in the synthesis gel limit the condensation of the inorganic walls. During calcination, the condensation of inorganic walls may be enhanced followed by contraction of unit cell size (12.8−11.8 nm), resulting in an increased pore diameter of the material. Moreover, it is shown that the pore size enlargement occurs without any ascertainable change in the structural order of the materials with increasing Al isopropoxide content in the synthesis gel. In addition, all materials prepared with various n_{Si}/n_{Al} ratios from 100 to 7 possess higher pore volumes as compared to those of the pure silica SBA-15 materials thus indicating in a high fraction of (ultra)micropores in the AlSBA-15 samples.[46,47] This indicates that AlSBA-15 materials can be prepared with very high aluminum content ($n_{Si}/n_{Al} = 7$) without affecting the structural order of the materials.

The ^{27}Al MAS NMR spectra of calcined AlSBA-15(7) and AlSBA-15(45) are shown in Figure 7. It can be seen that the coordination of Al was significantly affected with increasing n_{Si}/n_{Al} ratio in the product. All samples prepared up to the n_{Si}/n_{Al} ratio of 45 show only tetrahedral coordination. However, the coordination of the Al atoms is changed below the n_{Si}/n_{Al} ratio of 45. AlSBA-15(7) shows a sharp peak centered around 53 ppm and two small peaks centered around 7 and 22 ppm. The peak at 53 ppm is attributed to aluminum in tetrahedral coordination sphere. The peaks corresponding to 22 and 7 ppm

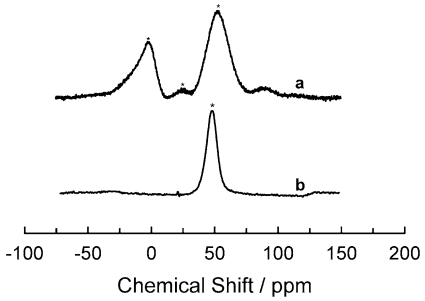

Figure 7. ^{27}Al MAS NMR spectra of AlSBA-15 materials prepared at different n_{Si}/n_{Al} ratios: (a) AlSBA-15(7) and (b) AlSBA-15(45).

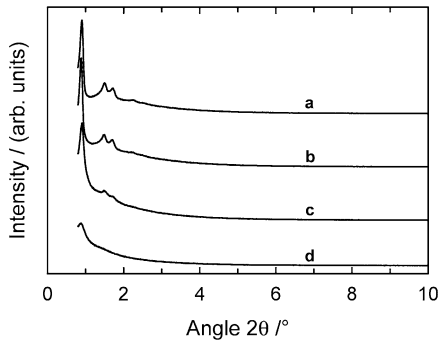

Figure 8. XRD powder patterns for the pressed AlSBA-15 materials: (a) AlSBA-15(0 MPa), (b) AlSBA-15(43 MPa), (c) AlSBA-15(107 MPa), and (d) AlSBA-15(217 MPa).

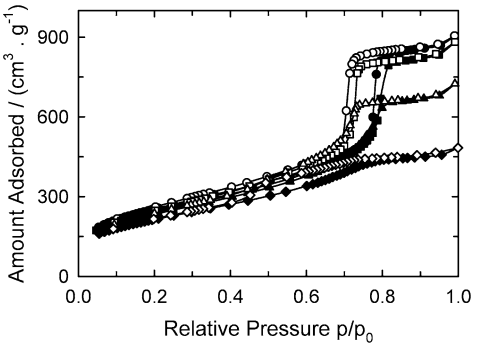

Figure 9. Nitrogen adsorption isotherms for the pressed AlSBA-15 materials (closed symbols, adsorption; open symbols, desorption): (●) AlSBA-15(0 MPa), (■) AlSBA-15(43 MPa), (▲) AlSBA-15(107 MPa), and (◆) AlSBA-15(217 MPa).

are attributed to penta- and hexacoordinated aluminum which might have formed by leaching during calcination. A similar behavior has also been reported for AlMCM-41 materials.[28−33]

Mechanical Stability of AlSBA-15. Figure 8 shows the powder X-ray diffraction patterns of the pressed samples in comparison to the parent AlSBA-15(0 MPa) material ($n_{Si}/n_{Al} = 45$). The quality of the material decreases slightly with increasing pelletizing pressure up to 107 MPa, while the structural order is lost after pressing at 217 MPa. With increasing pressure, the amount of adsorbed nitrogen also decreases (Figure 9). Moreover, there is no condensation step for the sample AlSBA-15(217 MPa), which indicates that the hexagonal pore structure is completely collapsed after compression at 217 MPa. A similar trend has also been observed for pure silica SBA-15.[47] Furthermore, with increasing pressure, specific pore volume and surface area decrease (Table 4). The BJH pore size distribution (not shown) was broadened with increasing pelletizing pressure, and no peak is obtained after pressing at 217 MPa, which confirm that the mesopores are completely destroyed after pressing at 217 MPa.

TABLE 4: Textural Parameters of the Pressed AlSBA-15 Materials

sample	pelletizing press./MPa	a_0/nm	A_{BET}/(m^2/g)	pore vol/(cm^3/g)	pore diam, $d_{p,ads}$/nm[a]	pore diam, $d_{p,Hg}$/nm[b]
AlSBA-15(0)	0	11.27	930	1.35	9.7	9.8
AlSBA-15(43)	43	11.53	893	1.29	10.2	10.9
AlSBA-15(107)	107	11.18	856	1.05	7.8	9.8
AlSBA-15(217)	217		783	0.71	1.4	9.7

[a] Pore diameter calculated from the nitrogen adsorption isotherm. [b] Pore diameter obtained from the mercury porosimetry analysis.

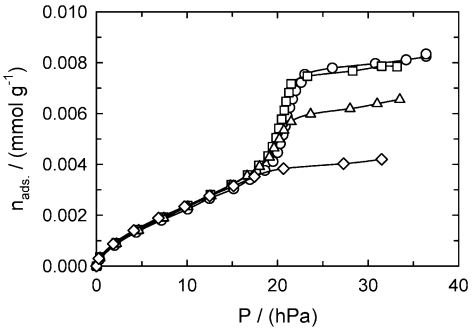

Figure 10. *n*-Heptane adsorption isotherms for the pressed AlSBA-15 materials: (○) AlSBA-15(0 MPa), (□) AlSBA-15(43 MPa), (△) AlSBA-15(107 MPa), and (◇) AlSBA-15(217 MPa).

To evaluate the accessibility of the AlSBA-15 pore system after compression to large probe molecule with relevance to catalysis, the adsorption of *n*-heptane has been investigated. *n*-Heptane adsorption isotherms of pressed and unpressed samples are shown in Figure 10. All isotherms are of type IV except for AlSBA-15(217 MPa). The total uptake of organics after the pore condensation is complete is used to calculate the total pore volume (Gurvich rule) accessible to *n*-heptane. The specific pore volumes were calculated from the amount adsorbed, assuming that the density of the adsorbed phase is equal to the density of bulk liquid at adsorption temperature. The pore volumes calculated from the uptake of *n*-heptane are lower as compared to the pore volumes obtained from nitrogen adsorption. In our previous studies on SBA-15, it was also found that the pore volumes calculated from *n*-heptane adsorption are almost 40% lower than the ones calculated from the nitrogen adsorption data.[46,47] However, in AlSBA-15, the pore volume calculated from *n*-heptane was only 16% lower than the ones determined from the nitrogen adsorption isotherm. Recently, Ribeiro Carrot et al.[48] reported that the density of the nitrogen in the pores is higher than the normal bulk density (from 0.808 to 0.84). If we consider the density of nitrogen in the pores is 0.84, then the pore volume from *n*-heptane was only 12% lower than the nitrogen pore volume. These results indicate that the amount of (ultra)micropores in AlSBA-15 is substantially lower as compared to the pure silica SBA-15.[46,47]

Moreover, upon compression at 217 MPa, the pore volume calculated from the nitrogen adsorption decreases by 47%, where as the pore volumes calculated from *n*-heptane by 51% (Figure 11a). But in the case of SBA-15, the pore volume determined by *n*-heptane adsorption is reduced by 43%, while the pore volume calculated from nitrogen adsorption is reduced by 40% by pressing at 260 MPa.[46,47] These results indicate that the mechanical stability of AlSBA-15 is lower than that of SBA-15. The lower mechanical stability of AlSBA-15 can be explained by the theoretical model of hexagonal honeycomb structure from the following equation:[49]

$$\sigma_c^* = {}^4/_3(t/a)^2\sigma_c \qquad (4)$$

where σ_c^* is the elasticity limit for a hexagonal honeycomb, t is the wall thickness, a is the unit cell parameter, and σ_c is the elasticity limit of bulk material (silica = 7200 MPa). From the equation, it is known that σ_c^* is directly proportional to t/a ratio. The value of t/a for AlSBA-15 was 0.16 and SBA-15 was 0.14. The σ_c^* of AlSBA-15 is 186 MPa whereas the σ_c^* of SBA-15 is 231 MPa (eq 4). These theoretical values are very well agreement with our experimental data. From the XRD patterns of SBA-15[46,47] and AlSBA-15, it can be seen that the structure of AlSBA-15 is completely destroyed after compression at 217 MPa, whereas the pore structure of SBA-15 still remains intact even after compression at 260 MPa. The same model was also very well suited for other mesoporous materials such as MCM-41 and MCM-41.[49,50] Moreover, such a model is also supported by the decrease of the relative pore volume (Figure 11b), which is independent from the molecule adsorbed (nitrogen or *n*-heptane). The observed almost linear decrease of the relative pore volume of AlSBA-15 under uniform compression might be explained in terms of successive compression of grains, where the stress is applied in the plane of hexagonal section.

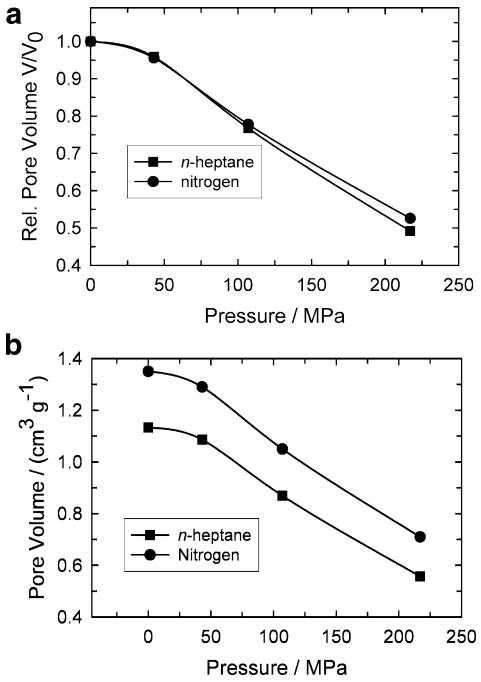

Figure 11. Comparison of (a) relative pore volume and (b) pore volume V/V_0 of AlSBA-15 determined by nitrogen (●) and *n*-heptane (■).

The textural properties of pressed AlSBA-15 materials were also characterized by mercury porosimetry (Figure 12). Mercury porosimetry is largely used to evaluate the porosity of industrial catalysts and other porous materials. Because of the high pressure needed to fill small pores, this method is at present limited to pores with $d_p > 3$ nm. In Figure 12, the pore size distribution of AlSBA-15 materials pressed at different pelletizing pressure are displayed. The pore diameter of AlSBA-15-(0 MPa) is determined to be 9.8 nm, in close agreement with the results from BJH analysis of the adsorption branch of the respective nitrogen isotherm (9.7 nm). It can be seen that the

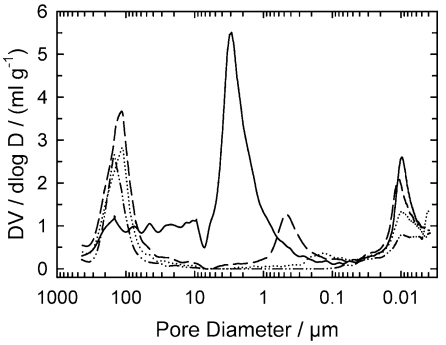

Figure 12. Pore size evalution by mercury porosimetry of AlSBA-15 samples compacted at different pressure: (—) AlSBA-15(0 MPa), (- - -) AlSBA-15(43 MPa), (· · ·) AlSBA-15(107 MPa), and (— · · —) AlSBA-15(217 MPa).

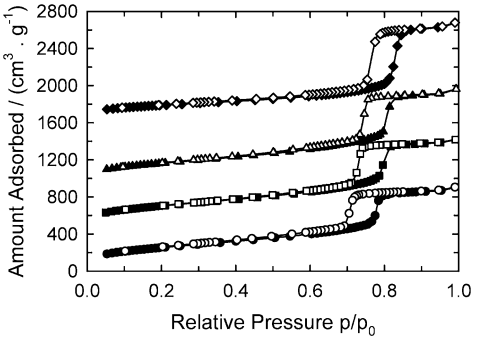

Figure 13. Nitrogen adsorption isotherms for the pressed AlSBA-15 materials (closed symbols, adsorption; open symbols, desorption): (●) AlSBA-15(100T), (■) AlSBA-15(110T), (▲) AlSBA-15(120T), and (◆) AlSBA-15(130T).

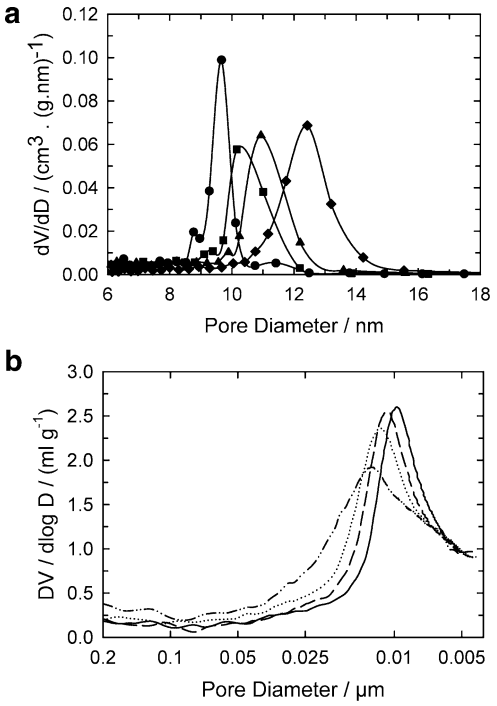

Figure 14. (a) BJH pore size distributions for the AlSBA-15 materials synthesized at different temperatures: (●) AlSBA-15(100T), (■) AlSBA-15(110T), (▲) AlSBA-15(120T), and (◆) AlSBA-15(130T). (b) Pore size evaluation by mercury porosimetry of AlSBA-15 samples synthesized at different temperatures: (—) AlSBA-15(100T), (- - -) AlSBA-15(110T), (· · ·) AlSBA-15(120T), and (— · · —) AlSBA-15(130T).

pore size distribution broadens with increasing pelletizing pressure. The second maximum around 5 μm is ascribed to the filling of the void spaces (macropores) between the primary particles. The study of the intergranular porosity shows that the particles are getting closer under pressure. Therefore, the size and the number of these pores decrease with increasing pelletizing pressure. For the pellets, a new maximum at ca. 100 μm is observed which represents the toroidal void space of a collection of solid particles.[51] The size of these macropores mainly depends on the pellet size and, hence, is independent of the pelletizing pressure and the catalyst under investigation.

Variation of the Synthesis Temperature. Recent studies[47,52] have shown that the pore diameter of SBA-15 materials can be increased by variation of the synthesis temperature between 100 and 130 °C. The XRD powder patterns of AlSBA-15 materials synthesized at different temperatures are very well-defined and characteristic of well-ordered hexagonal materials (Figure 3S, see Supporting Information). With increasing synthesis temperature, the XRD reflections are shifted to lower 2θ values, reflecting an expansion of the unit cell size (Table 5). It can be also seen that the relative intensity of the (110) and (200) refection shifts considerably; the intensity of the (110) reflection increases, whereas the intensity of the (200) reflection decreases. The more intense (110) peak in the AlSBA-15(130T) indicates that the material possesses thinner walls as suggested by Feuston et al.[53] for the analogous hexagonal structure of MCM-41. It is interesting to note that the structural order of the material is maintained up to the synthesis temperature of 130 °C. Moreover, it should be pointed out that the incorporation of aluminum was not affected by increasing the synthesis temperature (Table 5).

The nitrogen adsorption isotherms of the samples prepared at different synthesis temperature are shown in Figure 13. The position of the capillary condensation step shifts to higher relative pressure with increasing synthesis temperature. Moreover, as illustrated in Figure 11, the amount of N_2 adsorbed also increases with synthesis temperature. The textural properties obtained from examination of the nitrogen isotherms of AlSBA-15 prepared at different temperatures are summarized in Table 5. Specific pore volume (1.35−1.55 cm^3/g) and pore diameter (9.7−12.5 nm) increase with increasing synthesis temperature, whereas the surface area decreases from 930 to 600 m^2/g for samples prepared at synthesis temperature of 100 and 130 °C. The pore size distributions of AlSBA-15 samples synthesized at different temperature obtained from the nitrogen isotherm adsorption branch and from the Hg porosimetry are shown in parts a and b of Figure 14, respectively. The increase of pore diameter with the synthesis temperature was confirmed by Hg porosimetry. Figures 14a and 17b show that the pore size distribution of AlSBA-15 is uniform but broadens significantly

TABLE 5. Structural Parameters of AlSBA-15 Samples Prepared at Different Synthesis Temperature

sample	T_{syn}	a_0/nm	n_{Si}/n_{Al}	A_{BET}/(m^2/g)	pore vol/(cm^3/g)	pore diam, $d_{p,ads}$/nm[a]	pore diam, $d_{p,Hg}$/nm[b]
AlSBA-15(100T)	100	11.27	45	930	1.35	9.7	9.8
AlSBA-15(110T)	110	10.84	45	935	1.45	10.2	10.9
AlSBA-15(120T)	120	11.28	46	876	1.53	10.9	11.7
AlSBA-15(130T)	130	12.31	46	600	1.55	12.5	12.8

[a] Pore diameter calculated from the nitrogen adsorption isotherm. [b] Pore diameter obtained from the mercury porosimetry analysis.

with increasing synthesis temperature. Hg porosimetry also shows pore size ranging from 9.8 to 13 nm with increasing synthesis temperature, which is in close agreement with the nitrogen adsorption data (Table 5).

The increase of the pore diameter of AlSBA-15 with increasing synthesis temperature might be explained by changes to the nature of block copolymer with temperature. At low temperature, the poly(ethylene oxide) (PEO) chains of the micelle are hydrophilic in nature and the poly(propylene oxide) (PPO) chains are hydrophobic in nature. These PEO chains penetrate into the SBA-15 walls and interact via hydrogen bonds with the silanol groups. Hence it is believed that PEO chains are responsible for the formation of micropores in the SBA-15 framework.[8,47] With increasing synthesis temperature, the hydrophilicity of PEO chains decrease with concomitant increase of the hydrophobic character. This would probably enhance the interaction between the PPO chains of the micelle. As a result, the length of the hydrophobic part of the surfactant micelle increases (interaction between the PEO and PPO chains), and thus the micelle size increases with increasing synthesis temperature. These variations in micelle size are also reflected in a substantial broadening of the pore size distribution of the AlSBA-15 materials while increasing the temperature from 100 to 130 °C.

Conclusions

We developed a new method to incorporate aluminum atoms into the SBA-15 silica matrix with very high structural order and high aluminum content by simply adjusting the molar water to hydrochloric acid ratio in the gel mixture. It has been found that the n_{Si}/n_{Al} ratio of the AlSBA-15 materials can be controlled and prepared up to n_{Si}/n_{Al} ratio of 7 by varying the molar water to hydrochloric acid ratio and n_{Si}/n_{Al} ratio in the synthesis gel. XRD, nitrogen adsorption, and ^{27}Al MAS NMR studies confirm that Al isopropoxide was the preferred Al source among all Al sources studied and gives very good textural property and a higher amount of aluminum incorporation with tetrahedal coordination. It has also been found that the n_{Si}/n_{Al} ratio of the final products depends on the nature of the aluminum source. All these observations confirm that the nature of the aluminum source is a crucial factor in determining the amount of aluminum incorporation, location, and coordination of Al in the SBA-15 framework. The pore diameter of AlSBA-15 can be tuned, for the first time, from 9 to 13 nm by simply adjusting the crystallization temperature without addition of any organic swelling agents. The pore diameter of the materials was determined by both nitrogen adsorption and mercury porosimetry analysis. Furthermore, the mechanical stability of hexagonal AlSBA-15 materials was studied by applying different pelletizing pressures and subsequent characterization by XRD and N_2 adsorption. *n*-Heptane adsorption isotherms were recorded to evaluate the uptake of organics of the compressed materials. It has been found that mechanical stability of AlSBA-15 is lower compared to pure silica SBA-15 materials.

Acknowledgment. Financial support of this work by Deutsche Forschungsgemeinschaft (Ha2527/4-2) and Fonds der Chemischen Industrie is gratefully acknowledged. A. Vinu is grateful to Prof. Y. Bando and Special Coordination Funds for Promoting Science and Technology from the Ministry of Education, Culture, Sports, Science and Technology of the Japanese Government for the award of ICYS Research Fellowship, Japan.

Supporting Information Available: Nitrogen adsorption isotherms of AlSBA-15 materials prepared using different Al sources, XRD powder patterns of AlSBA-15 materials prepared at different Si/Al ratios, and the XRD powder patterns of AlSBA-15 materials synthesised at different temperatures. This material is available free of charge via the Internet at http://pubs.acs.org.

References and Notes

(1) Kresge, C. T.; Leonowicz, M. E.; Roth, W. J.; Vartuli, J. C.; Beck, J. S. *Nature (London)* **1992**, *359*, 710.
(2) Beck, J. S.; Vartuli, J. C.; Roth, W. J.; Leonowicz, M. E.; Kresge, C. T.; Schmitt, K. T.; Chen, C. T.; Olson, D. H.; Sheppard, E. W.; McCullen, S. B.; Higgins, J. B.; Schlenker, J. L. *J. Am. Chem. Soc.* **1992**, *114*, 10834.
(3) Corma, A. *Chem. Rev.* **1997**, *97*, 2373.
(4) Sayari, A. *Stud. Surf. Sci. Catal.* **1996**, *102*, 1.
(5) Le, Q. N. US Patent 5118894, 1992.
(6) Le, Q. N. US Patent 5232580, 1993.
(7) Sayari, A. *Chem. Mater.* **1996**, *8*, 1840.
(8) Zhao, D.; Huo, Q.; Feng, J.; Chmelka, B. F.; Stucky, G. D. *J. Am. Chem. Soc.* **1998**, *120*, 6024.
(9) Zhao, D.; Feng, J.; Huo, Q.; Melosh, N.; Fredrikson, G.; Chmelka, B.; Stucky, G. D. *Science* **1998**, 279.
(10) Ryoo, R.; Kim, J. M.; Shin, C. H. *J. Phys. Che*m. **1996**, *100*, 17718.
(11) Kim, S. S.; Zhang, W.; Pinnavaia, T. J. *Science* **1998**, *282*, 1032.
(12) Hwang, L. M.; Guo, W. P.; Deng, P.; Xue, Z. Y.; Li, Q. Z. *J. Phys. Chem. B* **2000**, *104*, 2817.
(13) Kloestra, K. R.; Bekkum, H. V.; Jansen, J. C. *Chem. Commun.* **1997**, 2281.
(14) Zhao, D.; Sun, J.; Li, Q.; Stucky, G. D. *Chem. Mater.* **2000**, *12*, 275.
(15) Yang, P.; Zhao, D.; Margolese, D.; Chmelka, B. F.; Stucky, G. D. *Chem. Mater.* **1999**, *11*, 2831.
(16) Yang, P.; Zhao, D.; Margolese, D.; Chmelka, B. F.; Stucky, G. D. *Nature (London)* **1998**, *396*, 152.
(17) Yue, Y.; Gédéon, A.; Bonardet, J.-L.; Melosh, N.; D' Espinose, J.-B.; Fraissard, J. *Chem. Commun.* **1999**, 1967.
(18) Luan, Z.; Hartmann, M.; Zhao, D.; Zhou, W.; Kevan, L. *Chem. Mater.* **1999**, *11*, 1621.
(19) Zhang, W.-H.; Lu, J.; Han, B.; Li, M.; Xiu, J.; Ying, P.; Li, C. *Chem. Mater.* **2002**, *14*, 3413.
(20) Cheng, M.; Wang, Z.; Sakurai, K.; Kumata, F.; Saito, T.; Komatsu, T.; Yashima, T. *Chem. Lett.* **1999**, 131.
(21) Luan, Z.; Maes, E. M.; van der Heide, P. A. W.; Zhao, D.; Czernuszewicz, R. S.; Kevan, L. *Chem. Mater.* **1999**, *11*, 3680.
(22) Luan, Z.; Bae, J. Y.; Kevan, L. *Chem. Mater.* **2000**, *12*, 3202.
(23) Murugavel, R.; Roesky, H. W. *Angew. Chem., Int. Ed. Engl.* **1997**, *109*, 4491.
(24) Han, Y.; Sun, Y.; Li, D.; Xiao, F.-S.; Liu, J.; Zhang, X. *Chem. Mater.* **2002**, *14*, 1144.
(25) Han, Y.; Xiao, F.-S.; Wu, S.; Sun, Y.; Meng, X.; Li, D.; Lin, S.; Deng, F.; Ai, X. *J. Phys. Chem. B* **2001**, *105*, 7963.
(26) Occelli, M. L.; Biz, S.; Auroux, A.; Ray, G. J. *Microporous Mesoporous Mater.* **1998**, *26*, 193.
(27) Badamali, S. K.; Sakthivel, A.; Selvam, P. *Catal. Today* **2000**, *63*, 291.
(28) Janicke, M.; Kumar, D.; Stucky, G. D.; Chemlka, B. F. *Stud. Surf. Sci. Catal.* **1994**, *84*, 243.
(29) Borade, R. B.; Clearfield, A. *Catal. Lett.* **1995**, *31*, 267.
(30) Luan, Z.; He, H.; Cheng C. F.; Zhou, W.; Klinowski, J. *J. Phys. Chem. B* **1995**, *99*, 1018.
(31) Reddy, K. M.; Song, C. *Catal. Lett.* **1996**, *36*, 103.
(32) Biz, S.; Occelli, M. L. *Catal. Rev.—Sci. Eng.* **1998**, *40*, 329.
(33) Reddy, K. M.; Song, C. *Catal. Today* **1996**, *31*, 197.
(34) Hartmann, M.; Bischof, C. *Stud. Surf. Sci. Catal.* **1998**, *117*, 249.
(35) Corma, A.; Navarro, M. T.; Perez-Pariente, *J. Chem. Soc., Chem. Commun.* **1994**, 147.
(36) Tanev, P. T.; Pinnavaia, T. *Chem. Mater.* **1996**, *8*, 2068.
(37) Brunisma, P. J.; Hess, N. J.; Bontha, J. R.; Liu, J.; Baskaran, S. *Mater. Res. Soc. Proc.* **1997**, *359*, 710.
(38) Sayari, A.; Liu, P.; Kruk, M.; Jaroniec, M. *Langmuir* **1997**, *13*, 2499.
(39) Imperor-Clerc, M.; Davidson, P.; Davidson, A. *J. Am. Chem. Soc.* **2000**, *122*, 11925.
(40) Evans, D. F.; Wennerstrom, H. *The Colloid Domain*; VCH: New York, 1994.
(41) Israelachvili, J. N.; Mitchell, D. J.; Ninham, B. W. *J. Chem. Soc., Faraday Trans. B* **1976**, *72*, 1525.
(42) Luan, Z.; He, H.; Zhou, W.; Cheng, C.-F.; Klinowski, J. *J. Chem. Soc., Faraday Trans.* **1995**, *91*, 2955.
(43) Laha, S. C.; Kumar, R. *Microporous Mesoporous Mater.* **2002**, *53*, 163.

(44) Hartmann, M.; Bischof, C., unpublished results.
(45) Zana, R. *Adv. Colloid Interfaces Sci.* **1995**, *57*, 1.
(46) Hartmann, M.; Bischof, C. *Prepr. Pap.—Am. Chem. Soc., Div. Pet. Chem.* **2001**, *46*, 23.
(47) Hartmann, M.; Vinu, A. *Langmuir* **2002**, *18*, 8010.
(48) Ribeiro Carrot, M. M. J.; Candeias, A. J. E.; Carrott, P. J. M.; Ravikovitch, P. I.; Niemark, A. V.; Sequeira, A. D. *Microporous Mesoporous Mater.* **2001**, *47*, 323.
(49) Hartmann, M.; Vinu, A. *Stud. Surf. Sci. Catal.* **2003**, *146*, 285.
(50) Galarneau, A.; Desplantier-Giscard, D.; Di Renzo, F.; Fajula, F. *Catal. Today* **2001**, *68*, 191.
(51) Mayer, R.; Stowe, R. A. *J. Phys. Chem.* **1966**, *70*, 3867.
(52) Galarneau, A.; Cambon, H.; Renzo, F. D.; Ryoo, R.; Choi, M.; Fajula, F. *New J. Chem.* **2003**, *27*, 73.
(53) Feuston, B. P.; Higgins, J. B. *J. Phys. Chem.* **1994**, *98*, 4459.